Supplementary Material for: Faster uphill relaxation in thermodynamically equidistant temperature quenches

Alessio Lapolla and Aljaž Godec
Mathematical bioPhysics Group, Max Planck Institute for Biophysical Chemistry, 37077 Göttingen, Germany

Abstract

In this Supplementary Material (SM) we present detailed derivations of the main results for the Gaussian-Chain and tilted single-file diffusion model presented in the main Letter, as well as several supplementary examples with figures. We also present counterexamples demonstrating that the uphill-downhill asymmetry is not universal as it vanishes in sufficiently asymmetric multi-well potentials. However, we establish generic conditions under which the asymmetry is obeyed. Finally, we also discuss the non-Markovian Mpemba effect.

GAUSSIAN CHAIN AND ORNSTEIN-UHLENBECK PROCESS

We consider a Gaussian Chain with N+1 beads with coordinates $\mathbf{R} = \{\mathbf{r}_i\}$ connected by harmonic springs with potential energy $U(\mathbf{R}) = \frac{1}{2}\sum_{i=1}^{N} |\mathbf{r}_i - \mathbf{r}_{i+1}|^2$. The overdamped Langevin equation governing the dynamics of a Gaussian Chain with N+1 beads connected by ideal springs with zero rest-length and diffusion coefficient D is given by the set of coupled Itô equations

$$\begin{aligned} d\mathbf{r}_1(t) &= [-\mathbf{r}_1(t) + \mathbf{r}(t)_2]dt + \sqrt{2D}\boldsymbol{\xi}_1(t) \\ d\mathbf{r}_i(t) &= [\mathbf{r}_{i-1}(t) - 2\mathbf{r}_i(t) + \mathbf{r}_{i+1}(t)]dt + \sqrt{2D}\boldsymbol{\xi}_i(t) \\ d\mathbf{r}_{N+1}(t) &= [-\mathbf{r}_{N+1}(t) + \mathbf{r}_N(t)]dt + \sqrt{2D}\boldsymbol{\xi}_{N+1}(t), \end{aligned} \tag{S1}$$

where $\boldsymbol{\xi}_i(t)$ stands for zero mean Gaussian white noise, i.e.

$$\langle \boldsymbol{\xi}_i(t) \rangle = 0, \qquad \langle \xi_{i,k}(t)\xi_{i,l}(t') \rangle = \delta_{kl}\delta(t-t'). \tag{S2}$$

It is straightforward to generalize these formulas to any reversible $3(N+1)$-dimensional Ornstein-Uhlenbeck process $\mathbf{R}(t) \equiv \{\mathbf{r}_i(t)\}$ with some $\mathbb{R}^{3(N+1)} \times \mathbb{R}^{3(N+1)}$ symmetric force matrix $\boldsymbol{\Xi}$ and potential energy function $U(\mathbf{R}) = \frac{1}{2}\mathbf{R}^T\boldsymbol{\Xi}\mathbf{R}$

$$d\mathbf{R}(t) = \boldsymbol{\Xi}\mathbf{R}(t)dt + \sqrt{2}d\mathbf{W}_t, \tag{S3}$$

where $d\mathbf{W}_t$ is the $3(N+1)$-dimensional super-vector of independent Wiener increments with zero mean and unit variance, $\mathbb{E}[dW_{i,t}dW_{j,t'}] = \delta_{i,j}\delta(t-t')$. In this super-vector/super-matrix notation the Gaussian is recovered by introducing $\mathbb{R}^{3(N+1)} \times \mathbb{R}^{3(N+1)}$ tridiagnal super-matrix $\boldsymbol{\Xi}$ with elements

$$\boldsymbol{\Xi}_{ii} = \mathbb{1}, \quad \boldsymbol{\Xi}_{ii+1} = \boldsymbol{\Xi}_{ii-1} = (-1 - 1^{\delta_{i,1}+\delta_{i,N+1}})\mathbb{1}, \tag{S4}$$

where $\mathbb{1}$ is the 3×3 identity matrix. This leads to the equations of motion presented in the Letter. Since $\boldsymbol{\Xi}$ is supposed to be symmetric these equations can be decoupled by diagonalizing $\boldsymbol{\Xi}$ i.e. by passing to normal coordinates $\mathbf{R} \to \mathbf{X} \equiv \{\mathbf{x}_i\}$:

$$\mathbf{A}^T\boldsymbol{\Xi}\mathbf{A} = \mathrm{diag}(\boldsymbol{\mu}) \tag{S5}$$

where the diagonal super-matrix has elements $\mathrm{diag}(\boldsymbol{\mu})_{kk} = \mu_k\mathbb{1}$. This yields eigenvalues μ_i and orthogonal super-matrices $(\mathbf{A})_{ij} \equiv A_{ij}\mathbb{1}$, where the ith row $A_{ij}, j = 0, \ldots, N$ corresponds to an eigenvector of the 1-dimensional contraction of $\boldsymbol{\Xi}$ (see e.g. Eq. (S4) for the Gaussian chain, i.e. $\boldsymbol{\Xi}_{ii} \to 1$ and $\boldsymbol{\Xi}_{ii-1} \to (-1 - 1^{\delta_{i,1}+\delta_{i,N+1}})$).

In the particular case of the Gaussian chain the eigenvalues and eigenvectors read

$$\mu_k = 4\sin^2\left(\frac{k\pi}{2(N+1)}\right), \qquad A_{ij} = \sqrt{\frac{2^{1-\delta_{j,0}}}{N+1}}\cos\left[\frac{(2i-1)j\pi}{2(N+1)}\right]. \tag{S6}$$

The back-transformation corresponds to $\mathbf{r}_i = \sum_{k=0}^{N} A_{ik}\mathbf{x}_k$. In normal coordinates the the potential energy reads $U(\mathbf{X}) = \frac{1}{2}\sum_{k=1}^{N}\mu_k\mathbf{x}_k^2$ while the corresponding Fokker-Planck equation for the evolution of the Green's function at a

temperature T, $G_T(\mathbf{x},t|\mathbf{x}_0)$, reads

$$\left[\partial_t - D\sum_{k=0}^{N}\left(\partial^2_{\mathbf{x}_k} + \beta\mu_k\partial_{\mathbf{x}_k}\mathbf{x}_k\right)\right]G_T(\mathbf{x},t|\mathbf{x}_0) = \delta(\mathbf{x}-\mathbf{x}_0), \tag{S7}$$

where $\beta = 1/k_{\mathrm{B}}T$. Note that we are interested only in internal dynamics and not on the center-of-mass dynamics, therefore we will henceforth ignore the $k=0$ contribution, as the zero mode with $\mu_0 = 0$ pertains only to the center-of-mass motion. Without any loss of generality we henceforth set $D=1$ and measure energies in units of $k_{\mathrm{B}}T_{\mathrm{eq}}$, where T_{eq} is the equilibrium (post-quench) temperature as defined in the manuscript. Moreover, since we are only interested in the evolution at temperature T_{eq}, we further express temperature relative to T_{eq}, i.e. $\tilde{T} \equiv T/T_{\mathrm{eq}}$, such that $\tilde{T}=1$ corresponds to T_{eq}. The stationary solution of Eq. (S7) corresponds to the Boltzmann-Gibbs density

$$P^{\mathrm{eq}}_{\tilde{T}}(\mathbf{X}) = \prod_{k=1}^{N}\left(\frac{\mu_k}{2\pi}\right)^{3/2}\exp\left(-\frac{\mu_k\mathbf{x}_k^2}{2\tilde{T}}\right). \tag{S8}$$

The probability density of $\mathbf{X}$ starting from an initial probability density function $P^{\mathrm{eq}}_{\tilde{T}}(\mathbf{X})$ is obtained from the Green's function via

$$P_{\tilde{T}}(\mathbf{X},t) = \int d\mathbf{X}_0 G_1(\mathbf{X},t|\mathbf{X}_0)P^{\mathrm{eq}}_{\tilde{T}}(\mathbf{X}_0), \tag{S9}$$

where

$$G_1(\mathbf{X},t|\mathbf{X}_0,0) = \prod_{k=1}^{N}\left(\frac{\mu_k}{2\pi(1-\mathrm{e}^{-2\mu_k t})}\right)^{3/2}\exp\left[-\frac{\mu_k}{2(1-\mathrm{e}^{-2\mu_k t})}\left(\mathbf{x}_k^2 - 2\mathbf{x}_k\cdot\mathbf{x}_{0k}\mathrm{e}^{-\mu_k t} + \mathbf{x}_{0k}^2\mathrm{e}^{-2\mu_k t}\right)\right], \tag{S10}$$

is the well-known Green's function of an Ornstein-Uhlenbeck process. Note that $\lim_{t\to\infty} G_{\tilde{T}}(\mathbf{X},t|\mathbf{X}_0,0) = P^{\mathrm{eq}}_{\tilde{T}}(\mathbf{X})$. The intergal Eq. (S9) can easily be performed analytically and yields

$$P_{\tilde{T}}(\mathbf{X},t) = \prod_{k=1}^{N}\left(\frac{\mu_k}{2\pi[1+(\tilde{T}-1)\mathrm{e}^{-2\mu_k t}]}\right)\exp\left(-\frac{\mu_k\mathbf{x}_k^2}{2[1+(\tilde{T}-1)\mathrm{e}^{-2\mu_k t}]}\right). \tag{S11}$$

Eq. (S11) can now be used to calculate the Kullback-Leibler divergence (Eq. (3) in the Letter) to yield the first of Eqs. (8) in the Letter. Furthermore, the average potential energy and the system's entropy are defined as

$$\langle U(t)\rangle_{\tilde{T}} \equiv \int d\mathbf{x} P_{\tilde{T}}(\mathbf{x},t)U(\mathbf{x}), \quad S_{\tilde{T}}(t) = -\int d\mathbf{x} P_{\tilde{T}}(\mathbf{x},t)\ln P_{\tilde{T}}(\mathbf{x},t) \tag{S12}$$

and read, upon performing the integration and introducing $\Lambda_k^{\tilde{T}}(t) \equiv 1 + (\tilde{T}-1)\mathrm{e}^{-2\mu_k t}$,

$$\langle U(t)\rangle_{\tilde{T}} = \frac{3}{2}\sum_{l=1}^{N}\Lambda_k^{\tilde{T}}(t), \quad S_{\tilde{T}}(t) = \frac{3}{2}\sum_{k=1}^{N}\left[1 - \ln\left(\frac{\mu_k}{2\pi\Lambda_k^{\tilde{T}}(t)}\right)\right]. \tag{S13}$$

In the projected, non-Markovian setting we are interested in the dynamics of an internal distance $d_{ij}(t) \equiv |\mathbf{r}_i(t) - \mathbf{r}_j(t)|$. In normal coordinates this corresponds to

$$d_{ij} \equiv |\mathbf{r}_i - \mathbf{r}_j| = \sum_{k=1}^{N}\left|(A_{ik} - A_{jk})\,\mathbf{x}_k\right|. \tag{S14}$$

By doing so we project out $3(N-1)$ latent degrees of freedom and track only d_{ij}. The 'non-Markovian Green's function', that is, the probability density of d_{ij} and time t given that the full system evolves from $P^{\mathrm{eq}}_{\tilde{T}}(\mathbf{X}_0)$ is defined as

$$\begin{aligned}
\mathcal{P}_{\tilde{T}}(d,t) &= \int d\Omega \int d\mathbf{X}_0\,\delta\Big(\sum_{k=1}^{N}[A_{ik}-A_{jk}]\mathbf{x}_k - \mathbf{d}\Big)G_1(\mathbf{X},t|\mathbf{X}_0,0)P^{\mathrm{eq}}_{\tilde{T}}(\mathbf{X}_0)\\
&= d^2\int_0^\infty dl_0 l_0^2\int d\Omega\int d\Omega_0\,\delta\Big(\sum_{k=1}^{N}[A_{ik}-A_{jk}]\mathbf{x}_k - \mathbf{d}\Big)\delta\Big(\sum_{k=1}^{N}[A_{ik}-A_{jk}]\mathbf{x}_{k,0} - \mathbf{l}_0\Big)G_1(\mathbf{X},t|\mathbf{X}_0,0)P^{\mathrm{eq}}_{\tilde{T}}(\mathbf{X}_0)\\
&\equiv \int_0^\infty dl_0\,\mathcal{P}_{\tilde{T}}(d,t,l_0;P^{\mathrm{eq}}_{\tilde{T}}),
\end{aligned} \tag{S15}$$

where we first project onto the vectors $\mathbf{d}$ and $\mathbf{d}_0$ and afterwards marginalize over all respective angles Ω and Ω_0. Note that the stept in line 2 of Eq. (S15) is actually not necessary but is preferable if one also wants to access the general non-Markovian two-point joint density $\mathcal{P}_{\tilde{T}}(d,t,d_0;P^{\rm eq}_{\tilde{T}})$. The calculation proceeds as follows.

We first preform two 3-dimensional Fourier transforms $\mathbf{d}_0 \to \mathbf{u}$ and $\mathbf{d} \to \mathbf{v}$:

$$\begin{aligned}\hat{\mathcal{P}}_{\tilde{T}}(\mathbf{u},t,\mathbf{v}_0;P^{\rm eq}_{\tilde{T}}) &\equiv \frac{1}{(2\pi)^6}\int d\mathbf{d}\mathrm{e}^{-i\mathbf{v}\cdot\mathbf{d}}\int d\mathbf{d}_0\mathrm{e}^{-i\mathbf{u}\cdot\mathbf{d}_0}\mathcal{P}_{\tilde{T}}(\mathbf{d},t,\mathbf{d}_0;P^{\rm eq}_{\tilde{T}})\\ &= \frac{1}{(2\pi)^6}\prod_{k=1}^{N}\exp\left[-\frac{\mathcal{C}^{ij}_k}{2\mu_k}(1+(\tilde{T}-1)\mathrm{e}^{-2\mu_k t})\mathbf{v}^2-\frac{\mathcal{C}^{ij}_k}{2\mu_k}\mathbf{u}^2-2\frac{\mathcal{C}^{ij}_k}{2\mu_k}\mathrm{e}^{-\mu_k t}\mathbf{v}\cdot\mathbf{u}\right],\end{aligned} \tag{S16}$$

where we have introduced the short-hand notation

$$\mathcal{C}^{ij}_k \equiv (A_{ik}-A_{jk})^2. \tag{S17}$$

Now we define, as in the main text, $\Lambda^{\tilde{T}}_k(t) \equiv 1+(\tilde{T}-1)\mathrm{e}^{-2\mu_k t}$ as well as

$$\mathcal{A}^{ij}_{\tilde{T}}(t) \equiv \sum_{k=1}^{N}\Lambda^{\tilde{T}}_k(t)\mathcal{C}^{ij}_k/2\mu_k, \quad \mathcal{B}^{ij}_{\tilde{T}}(t) \equiv \tilde{T}\sum_{k=1}^{N}\mathcal{C}^{ij}_k\mathrm{e}^{-\mu_k t}/2\mu_k, \tag{S18}$$

and rewrite Eq. (S16) as

$$\hat{\mathcal{P}}_{\tilde{T}}(\mathbf{u},t,\mathbf{v}_0;P^{\rm eq}_{\tilde{T}}) = \frac{1}{(2\pi)^6}\exp\left(-\mathcal{A}^{ij}_{\tilde{T}}(t)\mathbf{v}^2-\mathcal{A}^{ij}_{\tilde{T}}(0)\mathbf{u}^2-2\mathcal{B}^{ij}_{\tilde{T}}(t)\mathbf{v}\cdot\mathbf{u}\right), \tag{S19}$$

which can be easily inverted back to give

$$\mathcal{P}_{\tilde{T}}(\mathbf{d},t,\mathbf{d}_0;P^{\rm eq}_{\tilde{T}}) = (4\pi)^{-3}[\mathcal{A}^{ij}_{\tilde{T}}(t)\mathcal{A}^{ij}_{\tilde{T}}(0)-\mathcal{B}^{ij}_{\tilde{T}}(t)^2]^{-3/2}\exp\left(-\frac{1}{4}\frac{\mathcal{A}^{ij}_{\tilde{T}}(0)\mathbf{d}^2-2\mathcal{B}^{ij}_{\tilde{T}}(t)\mathbf{d}\cdot\mathbf{d}_0+\mathcal{A}^{ij}_{\tilde{T}}(t)\mathbf{d}_0^2}{\mathcal{A}^{ij}_{\tilde{T}}(t)\mathcal{A}^{ij}_{\tilde{T}}(0)-\mathcal{B}^{ij}_{\tilde{T}}(t)^2}\right). \tag{S20}$$

The marginalization is henceforth straightforward and yields

$$\begin{aligned}\mathcal{P}_{\tilde{T}}(d,t,d_0;P^{\rm eq}_{\tilde{T}}) &= \frac{(dd_0)^2\exp\left(-\frac{1}{4}\frac{\mathcal{A}^{ij}_{\tilde{T}}(0)\mathbf{d}^2+\mathcal{A}^{ij}_{\tilde{T}}(t)\mathbf{d}_0^2}{\mathcal{A}^{ij}_{\tilde{T}}(t)\mathcal{A}^{ij}_{\tilde{T}}(0)-\mathcal{B}^{ij}_{\tilde{T}}(t)^2}\right)}{2\pi[\mathcal{A}^{ij}_{\tilde{T}}(t)\mathcal{A}^{ij}_{\tilde{T}}(0)-\mathcal{B}^{ij}_{\tilde{T}}(t)^2]^{3/2}}\int_0^{\pi}d\cos\theta\exp\left(\frac{1}{2}\frac{dd_0\mathcal{B}^{ij}_{\tilde{T}}(t)\cos\theta}{\mathcal{A}^{ij}_{\tilde{T}}(t)\mathcal{A}^{ij}_{\tilde{T}}(0)-\mathcal{B}^{ij}_{\tilde{T}}(t)^2}\right)\\ &= \frac{dd_0}{2\pi\mathcal{B}^{ij}_{\tilde{T}}(t)}\frac{\exp\left(-\frac{1}{4}\frac{\mathcal{A}^{ij}_{\tilde{T}}(0)\mathbf{d}^2+\mathcal{A}^{ij}_{\tilde{T}}(t)\mathbf{d}_0^2}{\mathcal{A}^{ij}_{\tilde{T}}(t)\mathcal{A}^{ij}_{\tilde{T}}(0)-\mathcal{B}^{ij}_{\tilde{T}}(t)^2}\right)}{[\mathcal{A}^{ij}_{\tilde{T}}(t)\mathcal{A}^{ij}_{\tilde{T}}(0)-\mathcal{B}^{ij}_{\tilde{T}}(t)^2]^{1/2}}\sinh\left(\frac{1}{2}\frac{\mathcal{B}^{ij}_{\tilde{T}}(t)dd_0}{\mathcal{A}^{ij}_{\tilde{T}}(t)\mathcal{A}^{ij}_{\tilde{T}}(0)-\mathcal{B}^{ij}_{\tilde{T}}(t)^2}\right).\end{aligned} \tag{S21}$$

The probability density of d at time t after having started from an initial density $P^{\rm eq}_{\tilde{T}}(\mathbf{X}_0)$ (i.e. the pre-quench equilibrium) follows by simple integration and finally reads

$$\mathcal{P}_{\tilde{T}}(d,t) = \int_0^{\infty}dl_0\mathcal{P}_{\tilde{T}}(d,t,l_0;P^{\rm eq}_{\tilde{T}}) \equiv \frac{d^2}{2\sqrt{\pi}}\mathcal{A}^{ij}_{\tilde{T}}(t)^{-3/2}\mathrm{e}^{-d^2/4\mathcal{A}^{ij}_{\tilde{T}}(t)}, \tag{S22}$$

which is precisely Eq. (7) in the manuscript. The average potential of mean force, $\langle\mathcal{U}(t)\rangle_{\tilde{T}} \equiv -\langle\ln\mathcal{P}^{\rm eq}_1(d)\rangle_{\tilde{T}}$ and entropy, $\mathcal{S}_{\tilde{T}}(t) \equiv -\langle\ln\mathcal{P}_{\tilde{T}}(d,t)\rangle_{\tilde{T}}$ (in units of $k_{\rm B}T$), where $\langle f(d)\rangle_{\tilde{T}} \equiv \int dl\mathcal{P}_{\tilde{T}}(l,t)f(l)$, in turn read

$$\begin{aligned}\langle\mathcal{U}(t)\rangle_{\tilde{T}} &= \ln\left(2\sqrt{\pi}\mathcal{A}^{ij}_{\tilde{T}}(0)^{3/2}\right)-\mathcal{A}^{ij}_{\tilde{T}}(t)^{1/2}(2-\gamma_{\rm e}+\ln\mathcal{A}^{ij}_{\tilde{T}}(t))+\frac{3}{2}\frac{\mathcal{A}^{ij}_{\tilde{T}}(t)}{\mathcal{A}^{ij}_{\tilde{T}}(0)}\\ \mathcal{S}_{\tilde{T}}(t) &= \ln\left(2\sqrt{\pi}\mathcal{A}^{ij}_{\tilde{T}}(t)^{3/2}\right)-\mathcal{A}^{ij}_{\tilde{T}}(t)^{1/2}(2-\gamma_{\rm e}+\ln\mathcal{A}^{ij}_{\tilde{T}}(t))+\frac{3}{2}\end{aligned} \tag{S23}$$

where $\gamma_{\rm e}$ denotes Euler's gamma. Using the results in Eq. (S23) as well as the definition of the equilibrium free energy, $F = -\ln Q_1 \equiv -\ln\int d\mathbf{X}\mathrm{e}^{-U(\mathbf{X})}$, (where all potentials are in units of $k_{\rm B}T_{\rm eq}$) we arrive at

$$\mathcal{D}[P_{\tilde{T}}(t)||P_1] = \langle U_{\tilde{T}}(t)\rangle - S_{\tilde{T}}(t) - F, \quad \mathcal{D}[\mathcal{P}_{\tilde{T}}(t)||\mathcal{P}_1] = \langle\mathcal{U}^{\rm eff}_{\tilde{T}}(t)\rangle - \mathcal{S}_{\tilde{T}}(t), \tag{S24}$$

which are exactly Eqs. (4) and (5) in the Letter. For any stable symmetric matrix $\boldsymbol{\Xi}$ the condition of equidistant quenches $\mathcal{D}[P_{\tilde{T}^+}(0^+)||P_1] = \mathcal{D}[P_{\tilde{T}^-}(0^+)||P_1]$ is satisfied by

$$\tilde{T}^+ - \tilde{T}^- = \ln(\tilde{T}^+/\tilde{T}^-) \quad \rightarrow \quad \tilde{T}^+(\tilde{T}^-) = -W_{-1}(-\tilde{T}^- \mathrm{e}^{-\tilde{T}^-}), \tag{S25}$$

where $W_{-1}(x)$ defined for $x \in [-\mathrm{e}^{-1}, 0)$ denotes the second real branch of the Lambert-W function, which in turn satisfies the following sharp two-sided bound [1]

$$\frac{2}{3}\left[1 + \sqrt{2(\tilde{T}^- - 1 - \ln \tilde{T}^-)} + \tilde{T}^- - 1 - \ln \tilde{T}^-\right] \leq \tilde{T}^+(\tilde{T}^-) \leq 1 + \sqrt{2(\tilde{T}^- - 1 - \ln \tilde{T}^-)} + \tilde{T}^- - 1 - \ln \tilde{T}^-. \tag{S26}$$

Kullback-Leibler divergence and uphill/downhill asymmetry in relaxation of a random Gaussian network

In the Letter we prove that for any reversible ergodic Ornstein-Uhlenbeck process uphill relaxation (i.e. for a quench from $\tilde{T}^- \uparrow 1$ for which $\langle U(0^+)\rangle_{\tilde{T}^-} - \langle U\rangle_1 < 0$) is always faster that downhill relaxation (i.e. for a quench from $\tilde{T}^+ \downarrow 1$ for which $\langle U(0^+)\rangle_{\tilde{T}^-} - \langle U\rangle_1 > 0$), where the pair of equidistant quenches $\tilde{T}^+$ and $\tilde{T}^-$ is defined in the Letter. To visualize this on hand of an additional instructive example, we generated a random Gaussian network woth 10 beads by filling elements of the upper-triangular part of the connectivity matrix with a -1 according to a Bernulli distribution with $p = 0.7$. The resulting matrix was then symmetrized and the diagonal elements chosen to assure sure mechanical stability (i.e. 'connectedness'). The resulting connectivity matrix $\boldsymbol{\Gamma}$ is related to the general Ornstein-Uhlenbeck matrix in Eq. (S3) via $\boldsymbol{\Xi} = \boldsymbol{\Gamma} \otimes \mathbb{1}$, where

$$\boldsymbol{\Gamma} = \begin{pmatrix} 5 & -1 & -1 & 0 & -1 & 0 & 0 & 0 & -1 & -1 \\ -1 & 5 & -1 & 0 & -1 & -1 & 0 & 0 & 0 & -1 \\ -1 & -1 & 8 & -1 & -1 & 0 & -1 & -1 & -1 & -1 \\ 0 & 0 & -1 & 7 & -1 & -1 & -1 & -1 & -1 & -1 \\ -1 & -1 & -1 & -1 & 9 & -1 & -1 & -1 & -1 & -1 \\ 0 & -1 & 0 & -1 & -1 & 7 & -1 & -1 & -1 & -1 \\ 0 & 0 & -1 & -1 & -1 & -1 & 7 & -1 & -1 & -1 \\ 0 & 0 & -1 & -1 & -1 & -1 & -1 & 7 & -1 & -1 \\ -1 & 0 & -1 & -1 & -1 & -1 & -1 & -1 & 8 & -1 \\ -1 & -1 & -1 & -1 & -1 & -1 & -1 & -1 & -1 & 9 \end{pmatrix}. \tag{S27}$$

The corresponding results for $\mathcal{D}[\mathcal{P}_{\tilde{T}}(t)||\mathcal{P}_1]$, whereby we tagged the distance between the 1st and 10th bead, i.e. $d = |\mathbf{r}_1 - \mathbf{r}_{10}|$ are shown in Fig. S1.

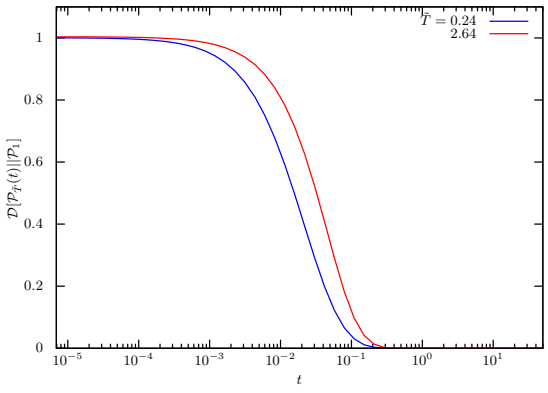

Figure S1. $\mathcal{D}[\mathcal{P}_{\tilde{T}^\pm}(t)||\mathcal{P}_1]$ as a function of time for a pair of equidistant quenches with $\tilde{T}^+ = 2.64$ and $\tilde{T}^- = 0.24$, which illustrates the asymmetry in the thermal relaxation holds for any Gaussian Network (according to our proof).

TILTED SINGLE FILE

We consider a system of N hard-core point-particles (the extension to a finite diameter is straightforward [2, 3]) diffusing in a box of unit length with a diffusion coefficient D, which we set equal to 1 and express energies in units of $k_{\rm B}T_{\rm eq}$ without any loss of generality. The particles with positions $\mathbf{x} = \{x_i\}$ feel the presence of a linear potential $U(\{x_i\}) = \sum_{i=1}^{N} g x_i$. The Green's function of the system obeys the many-body Fokker-Planck equation

$$(\partial_t - \hat{\mathcal{L}}_{\tilde{T}})G_{\tilde{T}}(\mathbf{x}, t|\mathbf{x}_0) \equiv \left(\partial_t - \sum_{i=1}^{N}(\partial_{x_i}^2 + g\tilde{T}^{-1}\partial_{x_i})\right) G_{\tilde{T}}(\mathbf{x}, t|\mathbf{x}_0) = \delta(\mathbf{x} - \mathbf{x}_0) \tag{S28}$$

The confining walls are assumed to be perfectly reflecting, i.e $J(x_i)|_{x_i=0} = J(x_i)|_{x_i=1} = -D(g/\tilde{T} - \partial_{x_i})G_{\tilde{T}}(\mathbf{x}, t|\mathbf{x}_0) = 0, \forall i$. Moreover, particles are not allowed to cross, which introduces the following set of internal boundary conditions

$$\left(\partial_{x_{i+1}} - \partial_{x_i}\right) G_{\tilde{T}}(\mathbf{x}, t|\mathbf{x}_0)|_{x_{i+1}-x_i=0} = 0, \forall i. \tag{S29}$$

Eq. (S28) with reflecting external boundary conditions $J(x_i)|_{x_i=0} = J(x_i)|_{x_i=1} = 0, \forall i$ and internal boundary conditions in Eq. (S29) is solved exactly using the coordinate Bethe ansatz (we do not repeat the results here as they can be found in [4]). It is convenient to introduce the particle-ordering operator

$$\hat{\mathcal{O}}_{\mathbf{x}} \equiv \prod_{i=2}^{N} \theta(x_i - x_{i-1}), \tag{S30}$$

where $\theta(x)$ is the Heaviside step-function. Let $\zeta_{\tilde{T}}(x_i, t|x_{0i})$ be the Green's function of the corresponding single-particle problem and $P^{\rm eq}_{\tilde{T}}(x_i) = \lim_{t\to\infty} \zeta_{\tilde{T}}(x_i, t|x_{0i})$ the density of the equilibrium measure at temperature $\tilde{T}$, then the Green's function can be written directly as

$$G_1(\mathbf{x}, t|\mathbf{x}_0) = N!\hat{O}_{\mathbf{x}} \prod_{i=1}^{N} \zeta_1(x_i, t|x_{0i}) \to P_{\tilde{T}}(\mathbf{x}, t) = N!\hat{O}_{\mathbf{x}} \prod_{i=1}^{N} \int_0^1 dx_{i0} \zeta_1(x_i, t|x_{i0}) P^{\rm eq}_{\tilde{T}}(x_{i0}), \tag{S31}$$

where the normalization factor $N!$ assures a correct re-weighing of non-crossing trajectories [4]. We expand the Green's function for a single particle at $\tilde{T} = 1$ in a bi-orthonormal eigenbasis, $\zeta(x, t|x_0) = \sum_k \phi_k^R(x)\phi_k^L(x_0)\mathrm{e}^{-\lambda_k t}$, where $\lambda_0 = 0$, $\lambda_k = \pi^2 k^2 + g^2/4$ and

$$\phi_k^L(x) = \frac{\mathrm{e}^{gx/2}}{\sqrt{2\lambda_k}} \left(g \sin(k\pi x) - 2k\pi \cos(k\pi x)\right), k > 0 \tag{S32}$$

and $\phi_k^R(x) = \mathrm{e}^{-gx}\phi_k^L(x)$, whereas for $k = 0$ we have $\phi_0^L(x) = 1$, $\phi_0^R(x) = P_1^{\rm eq}(x)$.

A key simplification in the calculation of order-preserving integrals as well as all projected, tagged-particle observables (incl. functionals; see e.g. [4]) is the so-called 'extended phase space integration' introduced by Lizana and Ambjörnsson [2, 3], according to which for any $1 \le M \le N$ and some function $f(\mathbf{x})$ that is symmetric with respect to permutation of coordinates x_i

$$\hat{O}_{\mathbf{x}} \prod_{i=1}^{N} \int_0^1 dx_{i0} f(\mathbf{x}) \delta(z - x_M) = \prod_{i=1}^{M-1} \int_0^z dx_{i0} \prod_{j=M+1}^{N} \int_z^1 dx_{j0} \frac{f(x_M = z, \{x_{i\neq M}\})}{(M-1)!(N-M)!}. \tag{S33}$$

With the aid of Eq. (S33) it is possible to calculate the Kullback-Leibler divergence as

$$\mathcal{D}[P_{\tilde{T}}||P_1] = \int d\mathbf{x} P_{\tilde{T}}(\mathbf{x}, t) \ln(P_{\tilde{T}}(\mathbf{x}, t)/P_1(\mathbf{x})) \equiv \left[\int_0^1 dx P^1_{\tilde{T}}(x, t) \ln(P^1_{\tilde{T}}(x, t)/P^1_1(x))\right]^N, \tag{S34}$$

where $P^1_{\tilde{T}}(x, t) = \int_0^1 dx_0 \zeta_1(x, t|x_0) P^{\rm eq}_{\tilde{T}}(x_0)$, and the second equality is a result of applying Eq. (S33). The result in Eq. (S34) for a single file of 10 particles is depicted in Fig. (3a) in the Letter. For the sake of completeness, we also present the exact explicit result for $\langle U(t)\rangle_{\tilde{T}} \equiv gN\langle x(t)\rangle_{\tilde{T}}$, which reads

$$\langle U(t)\rangle_{\tilde{T}} = gN\left(\frac{1 - \mathrm{e}^g + g}{g(1 - \mathrm{e}^g)} + 8\sum_{k=1}^{\infty}\left(\frac{gk\pi}{\lambda_k}\right)^2 \frac{(\tilde{T} - 1)(\mathrm{e}^{g/2} - (-1)^k)(\mathrm{e}^{g/\tilde{T}} - (-1)^k\mathrm{e}^{g/2})}{(\mathrm{e}^{g/\tilde{T}} - 1)[(\tilde{T} - 2)^2 g^2 + (2\pi k\tilde{T})^2]}\mathrm{e}^{-\lambda_k t}\right). \tag{S35}$$

The results for the non-Markovian tagged-particle dynamics can be derived analogously. The probability density function for tagging the Mth particle is defined as

$$\mathcal{P}_{\tilde{T}}(z,t) = \hat{\Pi}_{\mathbf{x}}(z) P_{\tilde{T}}(\mathbf{x},t) \equiv \hat{O}_{\mathbf{x}} \prod_{i=1}^{N} \int_0^1 dx_{i0} \delta(z - x_{\mathcal{T}}) P_{\tilde{T}}(\mathbf{x},t) \tag{S36}$$

and since $P_{\tilde{T}}(\mathbf{x},t)$ is symmetric to permutation of particle indices Eq. (S33) can be applied. The exact result has the form of a spectral expansion and reads

$$\mathcal{P}_{\tilde{T}}(z,t) = \sum_{\mathbf{k}} V_{0\mathbf{k}}(z) \mathcal{V}^{\tilde{T}}_{\mathbf{k}0} \mathrm{e}^{-\lambda_{\mathbf{k}} t}, \tag{S37}$$

where $\mathbf{k} = \{k_i\}$ is a N-tuple of non-negative integers and $\lambda_{\mathbf{k}} = \sum_{n=1}^{N} \lambda_{k_n}$ are Bethe eigenvalues of the operator $\hat{\mathcal{L}}_1 = \sum_{i=1}^{N} (\partial_{x_i}^2 + g\partial_{x_i})$ in a unit box under non-crossing conditions with $\lambda_0 = 0$ and $\lambda_{k_i} = \pi^2 k_i^2 + g^2/4, \forall k > 0$. Let $N_L = \mathcal{T} - 1$ and $N_R = N - \mathcal{T}$ be the total number of particles to the left and to the right of the tagged particle, respectively. Then $V_{0\mathbf{k}}(z)$ and $\mathcal{V}^{\tilde{T}}_{\mathbf{k}0}$ in Eq. (S37) are defined as

$$V_{0k}(z) = \frac{m_{\mathbf{k}}}{N_L! N_R!} \frac{2g\alpha}{\tilde{T}\Omega^g_{\tilde{T}}(0,1)} \sum_{\{k_i\}} T^1_{\mathcal{T}}(z) \prod_{i=1}^{N_L} L^1_i(z) \prod_{i=N_L+2}^{N} R^1_i(z) \tag{S38}$$

$$\mathcal{V}^{\tilde{T}}_{\mathbf{k}0} = \frac{N!}{N_L! N_R!} \frac{2g\alpha}{\tilde{T}\Omega^g_{\tilde{T}}(0,1)} \int_0^1 dz \sum_{\{k_i\}} T^{\tilde{T}}_{\mathcal{T}}(z) \prod_{i=1}^{N_L} L^{\tilde{T}}_i(z) \prod_{i=N_L+2}^{N} R^{\tilde{T}}_i(z) \tag{S39}$$

where $\alpha = \tilde{T}/(2-\tilde{T})$, $\Omega^g_{\tilde{T}}(x,y) \equiv \mathrm{e}^{-gx/\tilde{T}} - \mathrm{e}^{-gy/\tilde{T}}$, and $m_{\mathbf{k}} = \prod_i n_{k_i}!$ is the multiplicity of the Bethe eigenstate corresponding to the N-tuple $\mathbf{k}$, and the number n_{k_i} counts how many times the eigenindex k_i appears in the Bethe eigenstate [4]. In Eq. (S39) we have introduced the auxiliary functions

$$T^{\tilde{T}}_{\mathcal{T}}(z) = P^{\mathrm{eq}}_{\tilde{T}}(z) \frac{\mathrm{e}^{gx/2} \left(g \sin(k_{\mathcal{T}} \pi z) - 2k_{\mathcal{T}} \pi \cos(k_{\mathcal{T}} \pi z) \right)}{\sqrt{2\lambda_{k_{\mathcal{T}}}}}, \forall k_{\mathcal{T}} > 0 \tag{S40}$$

and $T^{\tilde{T}}_{\mathcal{T}}(z) = P^{\mathrm{eq}}_{\tilde{T}}(z)$ for $k_{\mathcal{T}} > 0$ where $P^{\mathrm{eq}}_{\tilde{T}}(z)$ is defined as

$$\mathcal{P}^{\mathrm{eq}}_{\tilde{T}}(z) = \frac{gN!}{N_L! N_R!} \frac{\Omega^g_{\tilde{T}}(0,z)^{N_L} \Omega^g_{\tilde{T}}(z,1)^{N_R}}{\tilde{T}\Omega^g_{\tilde{T}}(0,1)} \mathrm{e}^{-gz/\tilde{T}}, \tag{S41}$$

as well as

$$L^{\tilde{T}}_i(z) = \begin{cases} \Omega^g_{\tilde{T}}(0,z)/\Omega^g_{\tilde{T}}(0,1), & k_i = 0 \\ \lambda_{\sqrt{\alpha} k_i} \Phi^{g,\alpha}_{k_i}(0,z) + k_i \pi g \Psi^{g,\alpha}_{k_i}(0,z)(\tilde{T}-1)/(2-\tilde{T}), & k_i > 0 \end{cases}$$

$$R^{\tilde{T}}_i(z) = \begin{cases} \Omega^g_{\tilde{T}}(z,1)/\Omega^g_{\tilde{T}}(0,1), & k_i = 0 \\ \lambda_{\sqrt{\alpha} k} \Phi^{g,\alpha}_{k_i}(z,1) + k_i \pi g \Psi^{g,\alpha}_{k_i}(z,1)(\tilde{T}-1)/(2-\tilde{T}), & k_i > 0, \end{cases}$$

Note that $\lambda_{xk} \equiv \pi^2 (x k_i)^2 + g^2/4, \forall k > 0$, and $\sum_{\{k_i\}}$ denotes the sum over all possible permutations of $\mathbf{k}$ and the functions $\Phi^{g,\alpha}_k(x,y)$ and $\Psi^{g,\alpha}_k(x,y)$ are defined as

$$\Phi^{g,\alpha}_k(x,y) = \frac{\mathrm{e}^{-gx/2\alpha} \sin(k\pi x) - \mathrm{e}^{-gy/2\alpha} \sin(k\pi y)}{\lambda_{\alpha k} \sqrt{2\lambda_k}}$$

$$\Psi^{g,\alpha}_k(x,y) = \frac{\mathrm{e}^{-gx/2\alpha} \cos(k\pi x) - \mathrm{e}^{-gy/2\alpha} \cos(k\pi y)}{\lambda_{\alpha k} \sqrt{2\lambda_k}}. \tag{S42}$$

Details of the calculations can be found in [4]. The evaluation of Kullback-Leibler divergence, $S_{\tilde{T}}(t), \mathcal{S}_{\tilde{T}}(t)$ as well as $\langle \mathcal{U}(t) \rangle_{\tilde{T}}$ cannot be carried out analytically and we therefore resort to efficient and accurate numerical quadratures. The results are presented in Fig. (3) in the Letter.

We performed extensive systematic calculations for different values of g and N, various combinations of $\tilde{T}^{\pm}$ as well as for different choices for tagged particles. All these calculations gave the same qualitative picture – *without any exceptions 'uphill' relaxation was always faster.* However, we are not able to prove rigorously that this is indeed always the case. Therefore, for the single file the universally faster uphill relaxation is only a conjecture.

NON-EXISTENCE OF A UNIQUE RELAXATION ASYMMETRY IN MULTI-WELL POTENTIALS AND GENERIC CONDITIONS WHEN THE ASYMMETRY IS OBEYED

In the letter we demonstrated that the relaxation in single-well potentials is faster uphill than downhill. We have proven that this is always the case near stable minima and for any reversible Ornstein-Uhlenbeck process. Based on additional physical arguments we hypothesized that the asymmetry is a general feature of diffusion in single-well potentials. However, as we remarked in the Letter, it is not difficult to construct counterexamples proving that the asymmetry is *not* a general phenomenon in all reversible ergodic diffusion processes.

To that end we condider Markovian diffusion in rugged, multi-well potentials parametrized by

$$U(x) = e(ax^6 + bx^4 + cx^3 + dx^2), \tag{S43}$$

with some appropriately chosen constants a, b, c, d and e. Let the dynamics evolve according to $\hat{L}_{\tilde{T}} = \partial_x^2 - \tilde{T}^{-1}\partial_x F(x)$, where $F(x) = -6e(ax^5 + 4bx^3 + 3cx^2 + 2dx)$ in a finite domain $a \leq x \leq b$ with reflecting boundaries, and let the corresponding Green's function be the solution of the following initial-boundary value problem

$$(\partial_t - \hat{L}_{\tilde{T}})G_{\tilde{T}}(x,t|x_0) = \delta(x - x_0), \quad -(\partial_x - \tilde{T}^{-1}F(x))G_{\tilde{T}}(x,t|x_0)|_{x=a} = -(\partial_x - \tilde{T}^{-1}F(x))G_{\tilde{T}}(x,t|x_0)|_{x=b} = 0. \tag{S44}$$

We solve the Fokker-Plank equation so defined via the Method of Lines. The results for three distinct parameter sets is shown in Fig. (S2). We did not perform a systematic analysis of all the possible potentials. However, based

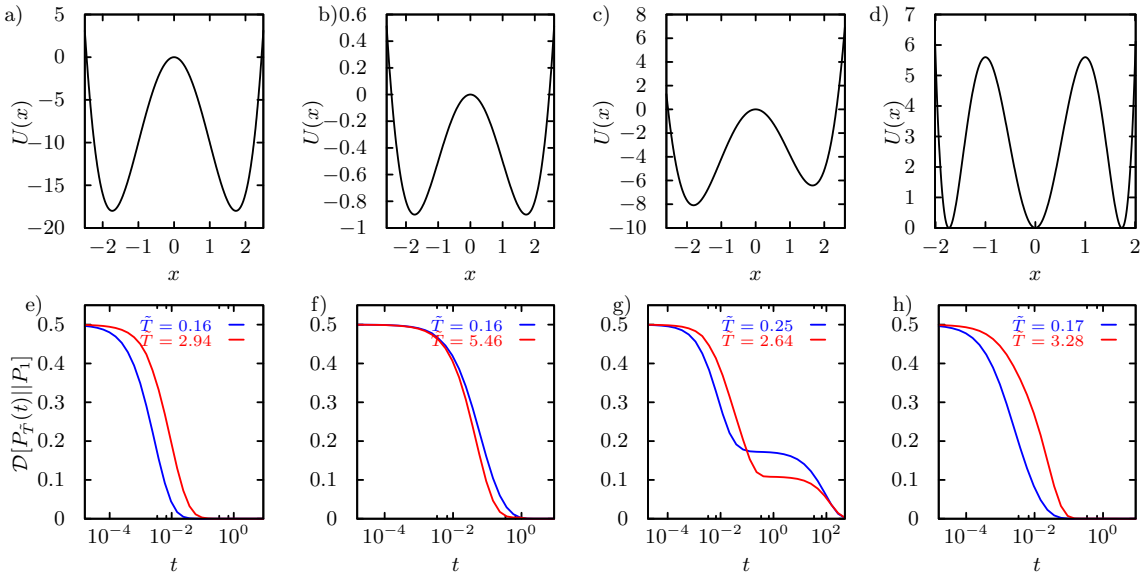

Figure S2. In panels a,b) and e,f) the potential is a quartic with parameter $a = 0, b = 1, c = 0, d = -6, e = 2$ in panels a and f and$a = 0, b = 1, c = 0, d = -6, e = 0.1$ in panels b and f. In the asymmetric potential in panels c and g with $a = 0, b = 1, c = 0.2, d = -6, e = 0.8$ and panels c and f with $a = 1, b = -6, c = 0, d = 9, e = 1.4$, respectively, the single-well asymmetry-pattern in fact becomes reversed. In a tripple-well with equally deep wells the asymmetry is again obeyed despite the middle well being wider.

on our observations it seems that the different uphill/downhill relaxation patterns depend on how different entropic contributions (i.e. intra-well entropy versus inter-well configuration entropy) change qualitatively with temperature for potentials with several minima.

If we focus on the asymmetric case (Fig. S2c) we find that uphill relaxation is initially always faster, which is a direct result of the physical mechanism at play that we present in the Letter. At longer time the asymmetry gets inverted by the slow inter-well partitioning of probability mass. It is now not diffcult to understand that by making the asymmetry smaller we will move the crossing point, where the corves intersect, closer to $\mathcal{D}[P_{\tilde{T}^{\pm}}(t)||P_1^{\text{eq}}] = 0$, such that for a sufficiently small asymmetry – which in the letter we refer to *near degeneracy* – uphill relaxation will eventually be faster for all times, for which $\mathcal{D}[P_{\tilde{T}^{\pm}}(t)||P_1^{\text{eq}}]$ differs from zero by an amount that is not neglgible/detectable. For a formal discussion of this situation see below.

It is interesting and important to note that the asymmetry is also obeyed if the barrier is moderately high, i.e. such that a small but non-neglible probability mass is located at the barrier (see Fig. S3). However, the quench must then not be too strong. That is, an 'infinitely' high barrier effecting a strict time-scale separation betwenn intra-well and inter-well relaxation is *not* a neccessarry condition for the asymmetry to occur. To demonstrate this we ispect overdamped relaxation according to Eq. (S44) in the following double well potential $U(x) = \Delta(x^2-1)^2$, where we choose (in units of $k_{\mathrm{B}}T_{\mathrm{eq}}$) $\Delta = 3$ and $F(x) = -U(x)'$.

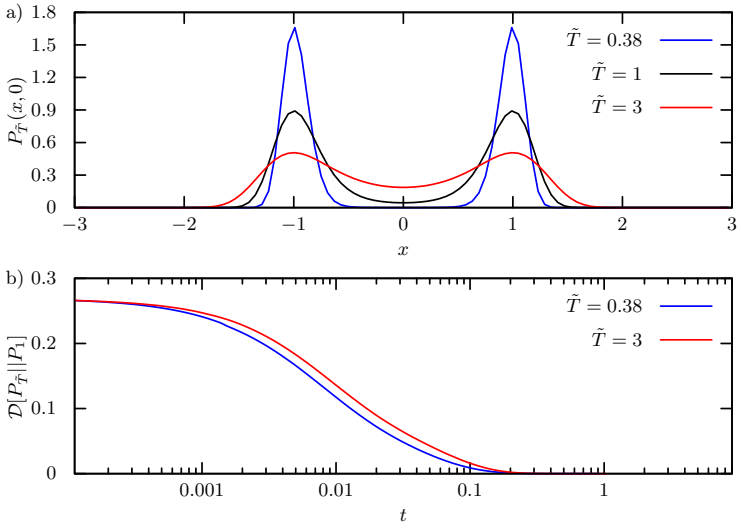

Figure S3. a) Density of invariant measure at $\tilde{T} = 1$ (i.e. equilibrium probability density), and the equidistant post-quench probability densities at $\tilde{T}^+ = 3$ and $\tilde{T}^- = 0.38$; b) Corresponding time evolution of the Kullback-Leibler divergence depicting that the asymmetry is obeyed.

In order to check that the observed effect in multi-well potentials is not an artifact of one-dimensional systems now also inspect 2-dimensional multi-well potentials. To that end we consider 4-well potentials parametrized by

$$U(x,y) = \Delta_x(x^2 - x_0^2)^2 + \Delta_y(y^2 - y_0^2), \tag{S45}$$

where energy is measured in units of $k_{\mathrm{B}}T_{\mathrm{eq}}$. We solve the problem by the *Alternating Direction Implicit* method (ADI) developed in [5] with 4-step operator splitting. We first focus on the limit of high barriers and quenches leaving the inter-well partitioning of probability mass unaffected (see Fig. S4). According to the proposed principle and prediction the symmetry is obeyes and uphill relaxation is always faster.

In Fig. S5 now inspect the case of a moderately high barriers (where the probability density on top of the barriers does not vanishes). As expected the asymmetry is obeyed only for sufficiently small quenches, whereas it becomes violated for stronger quenches (compare full and dashed lines). The reason for the violation is the fact that the inter-well redistribution becomes the dominant step for strong quenches.

It seems that the asymmetry observed in single-well potentials persists in nearly degenerate potentials and ceases to exists as soon as the potential becomes sufficiently asymmetric with sufficiently deep wells, where entropy attains an additional inter-well configurational component, such that during relaxation the probability mass becomes re-distributed between the wells in an asymmetric manner.

The asymmetry is obeyed in degenerate potentials in the presence of a time-scale separation

We now provide also formal arguments confirming that the symmetry must be obeyed in degenerate potentials in the presence of a time-scale separation. We follow the work of Moro [6]. Since we are dealing with systems obeying detailed balance the generator of the relaxation dynamics $\hat{\mathcal{L}}$ is always diagonalizable, i.e.

$$\hat{\mathcal{L}}_T = \sum_{k\geq 0} -\lambda_k \psi_k^R(\mathbf{x})\psi_k^L(\mathbf{x}_0) \tag{S46}$$

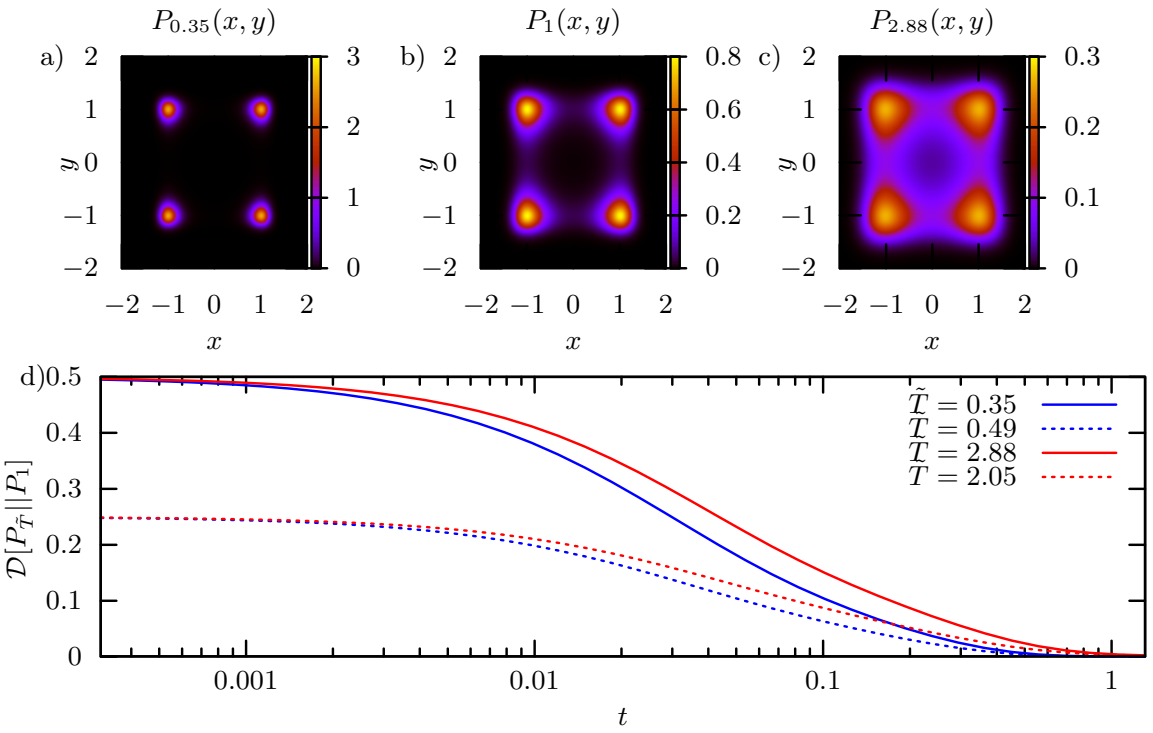

Figure S4. Density of invariant measure at $\tilde{T} = 1$ (b) (i.e. equilibrium probability density), and the equidistant post-quench probability densities at (c) $\tilde{T}^+ = 2.88$ and (a) $\tilde{T}^- = 0.35$ for the 4-well potential in Eq. (S45) with parameters $\Delta_x = \Delta_y = 3$ and $x_0 = y_0 = 1.$; d) Corresponding time evolution of the Kullback-Leibler divergence depicting that the asymmetry is obeyed for two pairs of equidistant temperatures.

where $\psi_k^R(\mathbf{x})$ and $\psi_k^L(\mathbf{x})$ are the orthonormal right and left eigenfunctions, respectively, (i.e. $\int \psi_k^L(\mathbf{x})\psi_l^R(\mathbf{x})d\mathbf{x} = \delta_{kl}$) and $-\lambda_k$ are real eigenvalues ($\lambda_0 = 0$ as we have assumed that the potential is confining and the dynamics is ergodic). The eigenfunctions constitute a complete bi-orthonormal basis, $\sum_k \psi_k^L(\mathbf{x})\psi_k^R(\mathbf{x}') = \delta(\mathbf{x} - \mathbf{x}')$. As a result of detailed balance we have $\psi_k^R(\mathbf{x}) = \mathrm{e}^{-U(\mathbf{x})/k_\mathrm{B}T}\psi_k^L(\mathbf{x})$ and $\psi_0^R(\mathbf{x}) = P_T^{\mathrm{eq}} \equiv \mathrm{e}^{-U(\mathbf{x})/k_\mathrm{B}T}/\int \mathrm{e}^{-U(\mathbf{x})/k_\mathrm{B}T}d\mathbf{x}$ and $\psi_0^L(\mathbf{x}) = 1$. Let $\hat{\mathcal{L}}_T^\dagger$ be the adjoint (or 'backward') generator, then we have the pair of eigenproblems $\hat{\mathcal{L}}_T\psi_k^R(\mathbf{x}) = -\lambda_k\psi_k^R(\mathbf{x})$ and $\hat{\mathcal{L}}_T^\dagger\psi_k^L(\mathbf{x}) = -\lambda_k\psi_k^L(\mathbf{x})$.

The Green's function of the relaxation problem, $(\partial_t - \hat{\mathcal{L}}_T)G_T(\mathbf{x}, t|\mathbf{x}_0) = 0$ with $G_T(\mathbf{x}, 0|\mathbf{x}_0) = \delta(\mathbf{x} - \mathbf{x}_0)$, decomposes to

$$G_T(\mathbf{x}, t|\mathbf{x}_0) = \sum_{k\geq 0} \psi_k^R(\mathbf{x})\psi_k^L(\mathbf{x}_0)\mathrm{e}^{-\lambda_k t} \rightarrow \quad P_{\tilde{T}}(\mathbf{x}, t) = \int G_1(\mathbf{x}, t|\mathbf{x}_0)P_{\tilde{T}}^{\mathrm{eq}}(\mathbf{x}_0)d\mathbf{x}_0. \tag{S47}$$

In presence of a time-scale separation (as a result of the existence of one or more high energy barriers) the eigenvalue spectrum of $\hat{\mathcal{L}}$ has a gap, i.e. $\exists k_{\min}$ such that $\lambda_{k_{\min}+l} \gg k_{\min} \forall l \geq 1$.

Assume now a set of M well-defined deep minima at $\hat{\mathbf{x}}_i, i = 1, \ldots, M$. This implies $k_{\min} = M - 1$. Let us define *localizing functions* $g_i(\mathbf{x}), i \in [1, M]$ such that

$$c_i^{\mathrm{eq}} \equiv \int g_i(\mathbf{x})P_1^{\mathrm{eq}}(\mathbf{x})d\mathbf{x} \quad \rightarrow \quad \int g_i(\mathbf{x})\psi_k^R(\mathbf{x}) = 0, \forall k \geq M, \tag{S48}$$

c_i^{eq} are the equilibrium site populations. The localizing functions therefore by definition separate the intra-well relaxation from the inter-well 'hopping' of probability mass. In turn this implies that $g_i(\mathbf{x})$ belong to the subspace $\{\psi_k^L(\mathbf{x})\}, k < M$, i.e.

$$g_i(\mathbf{x}) = \sum_{k=0}^{M-1} B_{ik}\psi_k^L(\mathbf{x}), \forall i \in [1, M] \tag{S49}$$

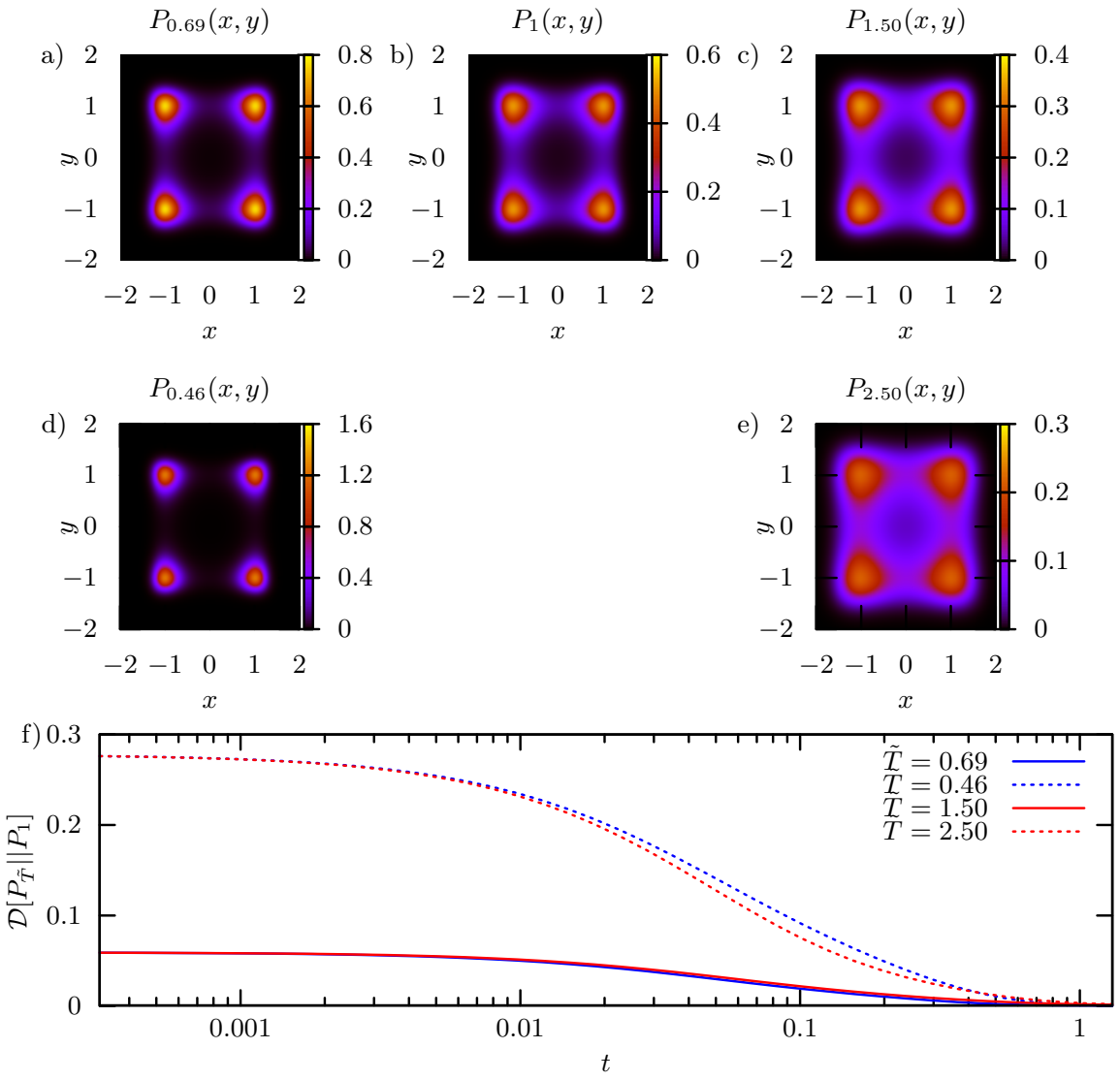

Figure S5. Density of invariant measure at (a) $\tilde{T}^- = 0.69$ (b) at $\tilde{T} = 1$, and at (c) $\tilde{T}^+ = 1.5$, (d) $\tilde{T}^- = 0.46$ and (e) $\tilde{T}^+ = 2.5$ corresponding to the 4-well potential in Eq. (S45) with parameters $\Delta_x = \Delta_y = 2$ and $x_0^2 = y_0^2 = 1$.; b) Corresponding time evolution of the Kullback-Leibler divergence depicting that the asymmetry is obeyed for small quenches (a and c) and violated for strong quenches (d and e).

and are thus by construction linearly independent but are so far only defined up to the expansion matrix $\mathbf{B}$. We determine $\mathbf{B}$ by imposing that the localizing functions should be localized near only one minimum $\hat{\mathbf{x}}_i$ and vanish at all remaining minima, i.e. $g_i(\hat{\mathbf{x}}_j) \simeq \delta_{i,j}$. Let the inverse of $\mathbf{B}$ be $\mathbf{B}^{-1}$, $\mathbf{B}^{-1}\mathbf{B} = \mathbb{1}$. We finally fix $g_i(\mathbf{x})$ by imposing the following resolution of identity $\sum_{I=1}^{M} g_i(\mathbf{x}) = 1$, which allows us to write

$$\psi_i^L(\mathbf{x}) = \sum_{k=1}^{M} B_{ik}^{-1} g_k(\mathbf{x}), \forall i \in [0, M-1], \tag{S50}$$

We now define the time-dependent population of the localizing sites (i.e. basins)

$$c_i(t) \equiv \int g_i(\mathbf{x}) G(\mathbf{x}, t|\mathbf{x}_0) d\mathbf{x}. \tag{S51}$$

The fact that $g_j(\mathbf{x})$ decompose unity implies that the total site population is conserved in time, i.e.

$$\sum_{i=1}^{M} c_i(t) \equiv \sum_{i=1}^{M} \int g_i(\mathbf{x}) G(\mathbf{x}, t|\mathbf{x}_0) d\mathbf{x} = \int \sum_{i=1}^{M} g_i(\mathbf{x}) G(\mathbf{x}, t|\mathbf{x}_0) d\mathbf{x} = 1, \tag{S52}$$

where we have used the fact that the integral and sum commute by Fubini's theorem (note that we can write the sum as an integral with respect to a counting measure). The localizing functions are linearly independent but not orthonormal. For this purpose we define the $M \times M$ superposition matrix $\mathbf{S}$ with elements $S_{ij} \equiv \int g_i(\mathbf{x}) P_1^{\mathrm{eq}}(\mathbf{x}) g_j(\mathbf{x}) d\mathbf{x}$ such that we can re-write the equilibrium site population as

$$c_i^{\mathrm{eq}} = \int g_i(\mathbf{x}) P_1^{\mathrm{eq}}(\mathbf{x}) \sum_{j=1}^{M} g_j(\mathbf{x}) d\mathbf{x} = \sum_{j=1}^{M} S_{ij}. \tag{S53}$$

We now define a projection operator projecting onto the space of localizing functions

$$\hat{\mathrm{P}} q(\mathbf{x}) \equiv \sum_{i=1}^{M} q_i g_i(\mathbf{x}), \quad q_i \equiv \sum_{k=1}^{M} S_{i,k}^{-1} \int g_i(\mathbf{x}) P_1^{\mathrm{eq}}(\mathbf{x}) q(\mathbf{x}) d\mathbf{x}. \tag{S54}$$

The time evolution of site populations then follows

$$\frac{dc_j(t)}{dt} = \int g_j(\mathbf{x}) \partial_t G_{\tilde{T}}(\mathbf{x}, t|\mathbf{x}_0) d\mathbf{x} = \int g_j(\mathbf{x}) \hat{\mathcal{L}}_1 G_{\tilde{T}}(\mathbf{x}, t|\mathbf{x}_0) d\mathbf{x} = \int G_{\tilde{T}}(\mathbf{x}, t|\mathbf{x}_0) \hat{\mathcal{L}}_1^{\dagger} g_j(\mathbf{x}) d\mathbf{x} \tag{S55}$$

$$\equiv \int G_{\tilde{T}}(\mathbf{x}, t|\mathbf{x}_0) \hat{\mathrm{P}} \hat{\mathcal{L}}_1^{\dagger} g_j(\mathbf{x}) d\mathbf{x} = \sum_{k,i} c_k(t) S_{k,i}^{-1} \int g_i(\mathbf{y}) \hat{\mathcal{L}}_1^{\dagger} P_1^{\mathrm{eq}}(\mathbf{y}) g_j(\mathbf{y}) d\mathbf{y} \equiv \sum_{k,i} c_k(t) S_{k,i}^{-1} \Gamma_{ij}, \tag{S56}$$

where in the second line we used the fact that $\hat{\mathcal{L}}_1^{\dagger} g_j(\mathbf{x})$ already lies in the subspace of localizing functions (because $\hat{\mathcal{L}}_T^{\dagger} \psi_k^L(\mathbf{x}) = -\lambda_k \psi_k^L(\mathbf{x})$ and Eq. (S49)) and the projection operator projects back onto said subspace. By defining $\mathbf{c}(t) = (c_i(t), \ldots, c_M(t))^T$ we recognize from Eq. (S56) that the site populations obey the Markovian master equation

$$\frac{d}{dt}\mathbf{c}(t) = \mathbf{M}\mathbf{c}(t), \quad M_{jk} \equiv \sum_i S_{k,i}^{-1} \Gamma_{ij}, \tag{S57}$$

where it can be shown that the transition rates entering $\mathbf{M}$ obey detailed balance [6]. It is obvious that $\mathbf{M}\mathbf{c}^{eq} = 0$ and therefore an equilibrated site-population does not lead to any inter-well dynamics. The evolution upon a temperature quench from $\tilde{T}$ follows from the evolution of the Green's function, i.e. $P_{\tilde{T}}(\mathbf{x}, t) = \int G_1(\mathbf{x}, t|\mathbf{x}_0) P_{\tilde{T}}^{\mathrm{eq}}(\mathbf{x}_0) d\mathbf{x}_0$. Therefore, any quench that will leave the site populations given the potential $U(\mathbf{x})$ and Fokker-Planck operator $\hat{\mathcal{L}}_1$ ($\hat{\mathcal{L}}_1^{\dagger}$ respectively) almost unaffected, i.e.

$$\mathbf{M}\mathbf{c}(0) \simeq 0, \quad \text{where} \quad c_i(0) = \int g_i(\mathbf{x}) P_{\tilde{T}}(\mathbf{x}, t=0|\mathbf{x}_0) d\mathbf{x} \equiv \int g_i(\mathbf{x}_0) P_{\tilde{T}}^{\mathrm{eq}}(\mathbf{x}_0) d\mathbf{x}_0, \tag{S58}$$

will lead to a faster uphill relaxation as a direct consequence of the fact that the intra-well (i.e. in each individual well) relaxation is faster uphill. The above arguments can be arranged in a form that is fully rigorous, but since the argumentation is essentially straightforward, we do not find it necessary to do so.

Small local modulations do not spoil the asymmetry

As stated in the Letter, small local modulations of the potential ($\ll k_{\mathrm{B}} T_{\mathrm{eq}}$) do not affect the asymmetry as longs as the uphill quench is sufficiently small to assure that the modulation is $\lesssim k_{\mathrm{B}} T^-$. Then the system relaxes similarly as in a perfectly smooth single well. To demonstrate that this is indeed the case we inspect the relaxation from equidistant quenches in the potential in Eq. (S45) with $\Delta_x = \Delta_y = 2$ and $x_0^2 = y^2 = 0.4$ depicted in Fig. S6. If, however, we make the quench too severe, such that the local modulations of the potential effectively reach $|\Delta U(\mathbf{x})| \gtrsim k_{\mathrm{B}} T^-$ the asymmetry would become violated and the curves will eventually cross, rendering downhill relaxation faster.

A a final example we focus on an asymmetric quadruple-well with a pair of high barriers and a pair of low barriers (the latter creating a small local modulation of the potential). In particular, we consider the relaxation in the potential

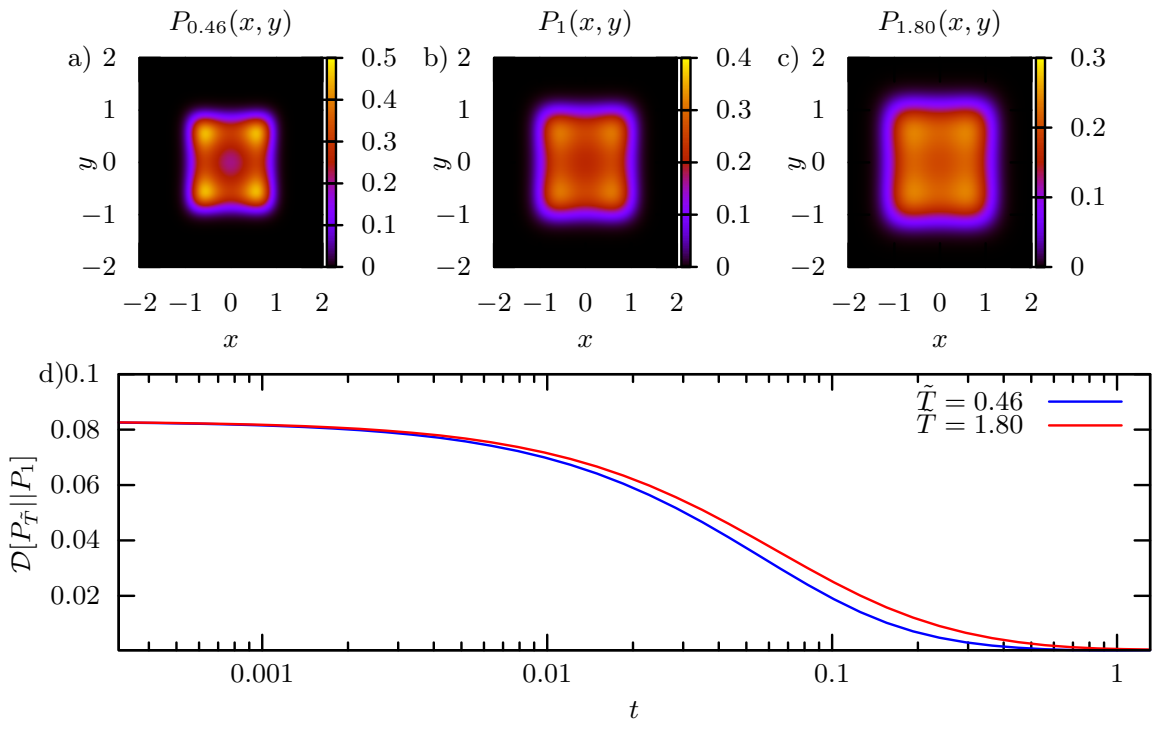

Figure S6. a) Density of invariant measure at $\tilde{T} = 1$ (i.e. equilibrium probability density), and the equidistant post-quench probability densities at $\tilde{T}^+ = 1.8$ and $\tilde{T}^- = 0.46$ for the 4-well potential in Eq. (S45) with parameters $\Delta_x = \Delta_y = 2$ and $x_0^2 = y_0^2 = 0.4$.; b) Corresponding time evolution of the Kullback-Leibler divergence depicting that the asymmetry is obeyed.

given in Eq. (S45) with parameters $\Delta_x = 3, \Delta_y = 2$ and $x_0 = 0.5, y_0 = 1$ and inspect in Fig. S7 the following pairs of thermodynamically equidistant temperatures, $\tilde{T}^- = 0.8, \tilde{T}^+ = 1.25$ and $\tilde{T}^- = 0.5, \tilde{T}^+ = 2.$.

As anticipated, the uphill relaxation is faster for sufficiently small quenches (see Fig. S7f) and becomes violated for stronger quenches (see Fig. S7g), where the Kullback-Leibler divergences also display an Mpemba-like effect (see also next section).

GENERALIZED MPEMBA EFFECT FOR NON-MARKOVIAN DYNAMICS

A phenomenon closely linked to relaxation from a quench is the so-called Mpemba effect [7–9], according to which a liquid upon cooling can freeze faster if its initial temperature is higher. Meanwhile the phenomenon has been extended to cover relaxation processes in different systems: magneto-resistors [10], carbon-nanotubes [11], polymers crystallization [12], clathrate hydrates [13], granular systems [14] and spin glasses [15]. Recently theoretical generalizations of it for Markovian observables have been published [16–18]. Not long ago the phenomenon was also adressed in more detail in the context of Markovian stochastic dynamics [16, 18].

Here we further extend the concept of the Mpemba effect to projected, non-Markovian observables. As before we focus on the distance of two different generic configurations displaced from equilibrium at $t = 0$, such that one is displaced further away than the other, whereas the time-evolution of the entire system is governed by the same Fokker-Planck operator. In this setting, there are cases, where the more distant initial configuration reaches equilibrium faster that the closer one. One can observe this effect in the two systems analyzed in the Letter (see Fig. S8). It is worth to stress that the presence of the generalized Mpemba effect not only depends on the system and the initial condition (like in the Markovian case) but also on the particular type of projection In Fig. S9 we demonstrate, on hand of the same system (a tilted single file of 5 particles) from the same pair of pre-quench temperatures, that we can switch the generalized Mpemba effect on and off by simply changing the particle we are tagging.

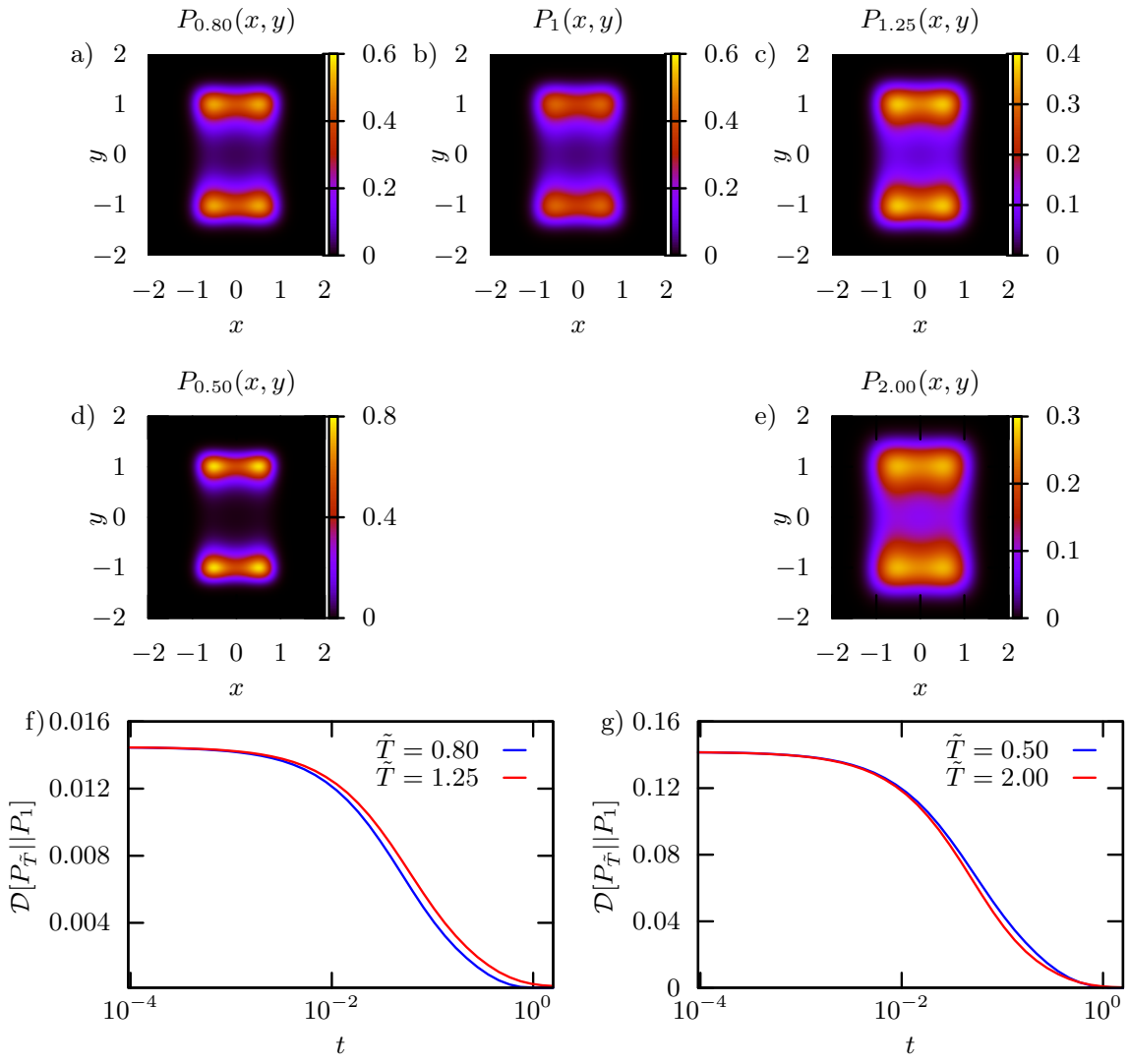

Figure S7. b) Density of invariant measure at $\tilde{T} = 1$ (i.e. equilibrium probability density), and two pairs of equidistant post-quench probability densities at $\tilde{T}^+ = 1.25$ (c) and 2 (e) and corresponding equidistant $\tilde{T}^- = 0.8$ (a) and 0.5 (d), respectively, for the 4-well potential in Eq. (S45) with parameters $\Delta_x = 3, \Delta_y = 2$ and $x_0 = 0.5, y_0 = 1.$; f-g) Corresponding time evolution of the Kullback-Leibler divergence depicting that the asymmetry is obeyed for small enough quenches but becomes violated (in the form of an Mpemba-like effect) for stronger quenches.

[1] I. Chatzigeorgiou, IEEE Communications Letters **17**, 1505–1508 (2013).
[2] L. Lizana and T. Ambjörnsson, Phys. Rev. E **80**, 051103 (2009).
[3] L. Lizana and T. Ambjörnsson, Phys. Rev. Lett. **100**, 200601 (2008).
[4] A. Lapolla and A. Godec, Front. Phys. **7** (2019), 10.3389/fphy.2019.00182.
[5] A. Godec, T. Ukmar, M. Gaberšček, and F. Merzel, EPL (Europhysics Letters) **92**, 60011 (2010).
[6] G. J. Moro, J. Chem. Phys. **103**, 7514–7531 (1995).
[7] E.B. Mpemba D.G. Osborne, Physics Education **14**, 410 (1979).
[8] M. Jeng, American Journal of Physics **74**, 514 (2006).
[9] J. I. Katz, American Journal of Physics **77**, 27 (2009).
[10] P. Chaddah, S. Dash, K. Kumar, and A. Banerjee, arXiv:1011.3598 [cond-mat, physics:physics] (2010), arXiv: 1011.3598.
[11] P. A. Greaney, G. Lani, G. Cicero, and J. C. Grossman, Metall and Mat Trans A **42**, 3907 (2011).
[12] C. Hu, J. Li, S. Huang, H. Li, C. Luo, J. Chen, S. Jiang, and L. An, Crystal Growth & Design **18**, 5757 (2018).
[13] Y.-H. Ahn, H. Kang, D.-Y. Koh, and H. Lee, Korean J. Chem. Eng. **33**, 1903 (2016).

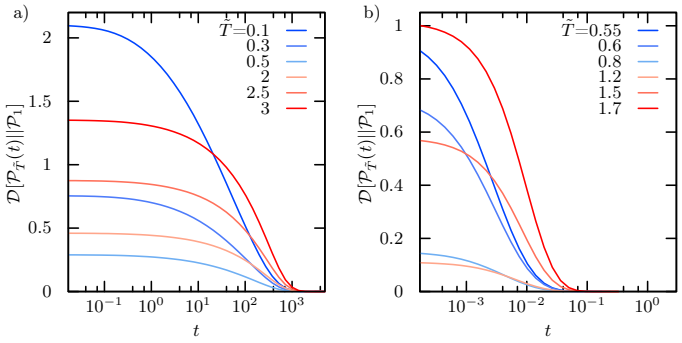

Figure S8. In the left panel we show time dependence of the Kullback-Leibler divergence for a Gaussian Chain of 100 beads, while the right panel depicts a Single File of 10 particles ($g = 5$). In both cases we focus on non-Markovian observables, the end-to-end distance for the Gaussian chain and on the 7th particle of the single file, respectively. For some pairs of initial temperatures we notice the generalized Mpemba effect: systems that start further away from the equilibrium approach the equilibrium configuration faster.

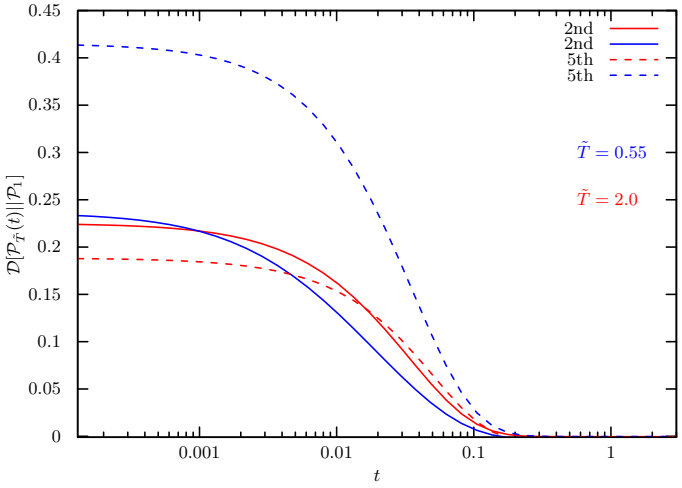

Figure S9. Kullback-Leibler divergences for a single file of 5 particles with $g = 1$. If we tag the 2nd particle (solid lines) or the 5th (dashed lines) for the same pair of pre-quench temperatures one projection displays the generalized Mpemba effect while the other one does not.

[14] A. Lasanta, F. Vega Reyes, A. Prados, and A. Santos, Phys. Rev. Lett. **119**, 148001 (2017).

[15] J. collaboration, M. Baity-Jesi, E. Calore, A. Cruz, L. A. Fernandez, J. M. Gil-Narvion, A. Gordillo-Guerrero, D. Iñiguez, A. Lasanta, A. Maiorano, E. Marinari, V. Martin-Mayor, J. Moreno-Gordo, A. Muñoz-Sudupe, D. Navarro, G. Parisi, S. Perez-Gaviro, F. Ricci-Tersenghi, J. J. Ruiz-Lorenzo, S. F. Schifano, B. Seoane, A. Tarancon, R. Tripiccione, and D. Yllanes, Proc Natl Acad Sci USA **116**, 15350 (2019),.

[16] Z. Lu and O. Raz, Proc Natl Acad Sci USA **114**, 5083 (2017).

[17] I. Klich and M. Vucelja, arXiv:1812.11962 [cond-mat, physics:math-ph] (2019), arXiv: 1812.11962.

[18] I. Klich, O. Raz, O. Hirschberg, and M. Vucelja, Phys. Rev. X **9**, 021060 (2019).